

Electronic properties of substitutional impurities in InGaN monolayer quantum wells

G. Alfieri, T. Tsutsumi, and R. Micheletto

Citation: [Applied Physics Letters](#) **106**, 192102 (2015); doi: 10.1063/1.4919787

View online: <http://dx.doi.org/10.1063/1.4919787>

View Table of Contents: <http://scitation.aip.org/content/aip/journal/apl/106/19?ver=pdfcov>

Published by the [AIP Publishing](#)

Articles you may be interested in

[Two-dimensional electron gas in monolayer InN quantum wells](#)

Appl. Phys. Lett. **105**, 213503 (2014); 10.1063/1.4902916

[The discrepancies between theory and experiment in the optical emission of monolayer In\(Ga\)N quantum wells revisited by transmission electron microscopy](#)

Appl. Phys. Lett. **104**, 182103 (2014); 10.1063/1.4875558

[Binding energies and oscillator strengths of impurity states in wurtzite InGaN/GaN staggered quantum wells](#)

J. Appl. Phys. **112**, 053525 (2012); 10.1063/1.4751438

[Donor impurity states in wurtzite InGaN staggered quantum wells](#)

Appl. Phys. Lett. **99**, 203110 (2011); 10.1063/1.3662848

[Influence of residual oxygen impurity in quaternary InAlGaIn multiple-quantum-well active layers on emission efficiency of ultraviolet light-emitting diodes on GaN substrates](#)

J. Appl. Phys. **99**, 114509 (2006); 10.1063/1.2200749

The advertisement features a dark blue background with three images: a mobile phone, a desktop computer, and an AFM. Text on the left asks 'You don't still use this cell phone' and 'or this computer'. Text in the center asks 'Why are you still using an AFM designed in the 80's?'. Text on the right promotes an upgrade to a new AFM, offering a \$20,000 trade-in discount for purchases before August 31st. The Oxford Instruments logo and tagline 'The Business of Science' are at the bottom right.

You don't still use this cell phone

or this computer

Why are you still using an AFM designed in the 80's?

It is time to upgrade your AFM

Minimum \$20,000 trade-in discount for purchases before August 31st

Asylum Research is today's technology leader in AFM

dropmyoldAFM@oxinst.com

OXFORD
INSTRUMENTS
The Business of Science®

Electronic properties of substitutional impurities in InGaN monolayer quantum wells

G. Alfieri,^{1,a)} T. Tsutsumi,² and R. Micheletto²

¹Department of Electronic Science and Engineering, Kyoto University, Kyotodai-gaku-katsura, Nishikyo, Kyoto 615-8510, Japan

²Department of Materials System Science, Yokohama City University, Yokohama 236-0027, Japan

(Received 12 November 2014; accepted 24 April 2015; published online 12 May 2015)

InGaN alloys and, in particular, InGaN monolayer quantum wells (MLQWs) are attracting an increasing amount of interest for opto-electronic applications. Impurities, incorporated during growth, can introduce electronic states that can degrade the performance of such devices. For this reason, we present a density functional and group theoretical study of the electronic properties of C, H, or O impurities in an InGaN MLQW. Analysis of the formation energy and symmetry reveals that these impurities are mostly donors and can be held accountable for the reported degradation of InGaN-based devices. © 2015 AIP Publishing LLC. [<http://dx.doi.org/10.1063/1.4919787>]

Nitride alloys have the ability to cover a wide range of wave-lengths of the electromagnetic spectrum, due to the variety of band gap values of GaN or AlN or InN. This is also the case for $\text{In}_x\text{Ga}_{1-x}\text{N}$, for which it is possible to tune the direct band gap (E_{GAP}) according to the In concentration x .^{1,2} Although there is no agreement on the E_{GAP} value, density functional theory calculations have shown that it varies between 3.3 and 2.1 eV for $x=0$ to 1.2–0.0 eV for $x=1$,¹ according to the calculation methodology employed. Typically, InGaN/GaN multiple quantum wells (MQWs)^{3,4} or InGaN/InN MQW⁵ are synthesized for LED applications. Yet, it is difficult to obtain high quality InGaN for this purpose, due to the high defect concentration arising from the lattice mismatch between InN and GaN. For this reason, molecular beam epitaxy (MBE) growth of an InGaN mono-layer quantum well (MLQW),^{6,7} that is a layer of InN embedded inside GaN, could overcome this issue.

Metal-organic precursors typically lead to C, H, and O incorporation into group III nitrides and, for this reason, their effect in GaN and InN has been thoroughly studied. It is known that C impurities reside in an N-substitutional position (C_N) in both GaN⁸ and InN,⁹ where it behaves as a shallow acceptor at 0.2–0.3 eV above the edge of the valence band, E_V . Hydrogen substitutes N in both GaN¹⁰ and InN¹¹ and behaves instead as donor. In GaN, hydrogen is known to effectively passivate Mg dopants,¹² whereas H behaves as a double donor in both p - and n - type InN.¹¹ Similarly to C and H, also oxygen prefers to sit at a N-site and behaves as a donor in both GaN¹³ and InN.⁹

Since the presence of impurities can give rise to electrically active levels in E_{GAP} , these can be detrimental for opto-electronic applications, e.g., passivation of dopants or charge carrier compensation, the following question arises: What is the effect of the presence of C, H, and O on the electronic properties of $\text{In}_x\text{Ga}_{1-x}\text{N}$ alloys? Or, more specifically, how do these impurities behave in an InGaN MLQW?

To answer this question, we present an *ab initio* investigation of the electronic properties of the C, H, and O isolated

substitutional impurities in InGaN MLQW, modeled using a 108-atom wurtzite GaN supercell, in which a layer of Ga atoms was substituted with In atoms (see Fig. 1(a)). Each of the three impurities was placed in the InN bilayer, by substituting a N atom with either a C (C_N), H (H_N), or O (O_N). The reason for this is that according to the literature, an N-site is the most energetically favorable site for C, H, and O. The siesta¹⁴ code was employed for carrying out the density functional theory calculations, by using Troullier-Martins norm-conserving pseudopotentials,¹⁵ to account for the effect of core electrons, and the Ceperley-Alder form of the local density approximation (LDA),¹⁶ for the exchange correlation potential. A double- ζ plus polarization was used as atomic orbitals basis set throughout the calculations. For the Ga and In atoms, the d -orbital electrons were treated as valence electrons. This choice was tested on wurtzite GaN and InN, respectively. For GaN, the $a=b$ and c lattice constants were both 1% larger than the experimental value with a direct band gap of 2.1 eV. For InN, the $a=b$ and c lattice constants were 0.3% larger than the experimental value and the calculated direct band gap was 0.2 eV. The equilibrium configurations of the pristine and defected InGaN MLQWs were obtained by relaxing the atomic coordinates with a conjugate

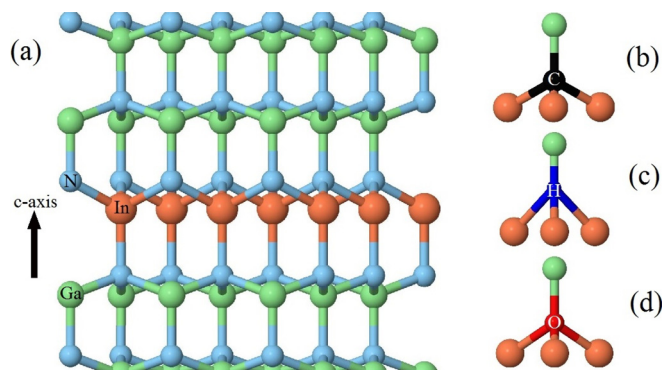


FIG. 1. Relaxed structure of the (a) InN MLQW embedded in the wurtzite GaN matrix and relaxed structures of the three (b) C, (c) H, and (d) O impurities in a N-substitutional site bonded to three In atoms and one Ga atom. Ga atoms are green, N atoms are light blue, In atoms are orange, C atom is black, H atom is blue, and O atom is red.

^{a)}Present address: ABB Corporate Research Center, Switzerland.

gradient algorithm, until the maximum atomic forces were less than 0.025 eV/Å and the stress tensor less than 0.5 GPa. The charge density was projected onto a real space grid with an equivalent cutoff of 400 Ry, while 4 Monkhorst-Pack special k-points¹⁷ ensured the convergence of the calculations.

After geometry relaxation (Fig. 1(a)), the In-N bonds, for In and N atoms lying in the same layer, become 2.04 Å, whereas In-N bonds between atoms in adjacent layers become 2.18 Å, in good agreement with the values obtained by Miao *et al.*² When C_N is present in the MLQW (Fig. 1(b)), the In- C_N bond length does not change significantly (2.04–2.05 Å) after geometry relaxation neither does the C_N -Ga bond (1.90 Å). These similarities are no surprise as the size of the C atom is similar to that of the N atom, thus introducing no or little strain in the InGaN MLQW. By replacing a N atom with hydrogen (H_N , Fig. 1(c)), geometry relaxation results in the displacement of the H atom from its substitutional site. The H atom ends up located along the c -axis halfway between the GaN (H-Ga bond length 1.52 Å) and InN (H-In bond length 2.23–2.25 Å) layers. The reason for this may be that, in both GaN and InN, H is more stable in an interstitial site rather than in a substitutional site.^{10,18} Similarly to the case of C, also the introduction of oxygen (O_N , Fig. 1(d)) results in a small strain between the GaN and InN bilayer, possibly due to the fact that O, like C, has a comparable size to N. After geometry relaxation, the O-Ga bond length is 1.9 Å whereas O-In is 2.1 Å.

In Fig. 2, we show the total and partial density of states of the InGaN MLQW, both pristine and in the presence of impurities. It can be seen (Fig. 2(a)) that the Kohn-Sham E_{GAP} is 1.2 eV, much lower than what is obtained by hybrid functional calculations.² In addition, we find that the top of the valence band (E_V) has mainly a p -character, arising from the p orbitals of the N atoms, while the contributions of the Ga (p, d orbitals) and In (p orbital) become more relevant deeper in the valence band. On the other side, the bottom of the conduction band (E_C) is mainly due to both s and p orbitals of N and, in about equal parts, to the s orbitals of both Ga and In. We point out that the predominance of N p -character in the valence band and the intermixing of N s and p orbitals in the conduction band is similar to what has been reported for bulk wurtzite GaN.¹⁹ The same pattern applies to the valence and conduction bands of an InGaN MLQW in the

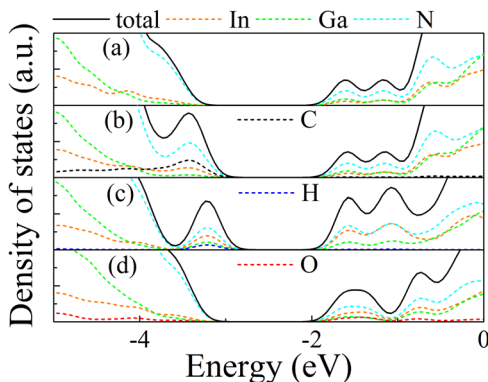


FIG. 2. Total (solid line) and partial (dashed lines) density of states for the (a) pristine InGaN MLQW, (b) InGaN MLQW with C_N , (c) InGaN MLQW with H_N , and (d) O_N .

presence of C. However, as shown in Fig. 2(b), a shallow state close to E_V and due to the p orbital of C can be found. Similarly, the s orbital of H is responsible for the presence of another shallow state close to the valence band (Fig. 2(c)). On the other side, O is not found in the vicinity of the valence band but it gives rise to a state (s and p character) inside the conduction band of InGaN, at 0.2–1 eV above E_C (Fig. 2(d)).

In order to understand how these states can affect the electronic properties of an InGaN MLQW, we calculated the formation energy (E_{form}), in the charge state q , of C_N , H_N , or O_N . This allows us to both evaluate the abundance of these impurities in the InN bilayer of wurtzite GaN, their acceptor or donor character as well as to obtain the respective ionization levels. E_{form} was calculated by employing the formalism of Zhang-Northrup²⁰ and, since the three impurities occupy a N-site, E_{form} becomes

$$E_{form} = E_{q,tot} - E_{bulk,tot} - \mu_X + \mu_N + q(E_F + E_V), \quad (1)$$

where $E_{q,tot}$, $E_{bulk,tot}$, μ_X , μ_N , and E_F are the total energies of defected, bulk InN/GaN system, the chemical potential of the substitutional impurity (C, H, or O), the chemical potential of the substituted N atom, and the Fermi level, respectively. We point out that the underestimation of E_{GAP} affects the calculated values of E_{form} and the use of hybrid functionals or other correction schemes can help to overcome this issue. For instance, the scissor operator *a-posteriori* correction²¹ would yield an increase of E_{form} of O_N of about 1.8 eV. Yet, the scissor operator described in Ref. 21 affects states close to the conduction band and, as we shall see, it does not provide a correction to the E_{form} of C_N and H_N . In addition, the validity of the scissor operator has not been proven for InGaN or other nitride alloys. For these reasons, we will report on the LDA-based results without the application of any correction scheme.

In the present study, we are interested in the incorporation of impurities in InN MLQW embedded in the GaN matrix. As described in Ref. 6, In-rich conditions are necessary not only for the synthesis of said InN MLQW⁶ but also promote the incorporation of C, H, and O impurities. For these reasons, the calculation of E_{form} will be carried out by considering In-rich (or N-poor) conditions. This means that in the case of an InN MLQW

$$\mu_{In(InN)} + \mu_{N(InN)} = \mu_{InN(bulk)}, \quad (2)$$

where the chemical potential of bulk InN is given by the sum of the chemical potential of In and N in InN, respectively. Under In-rich conditions, $\mu_{In[InN]} = \mu_{In[bulk]}$ and, at the same time, $\mu_{N[InN]} = \mu_{InN[bulk]} - \mu_{In[bulk]}$ which is also equal to $\mu_{N[bulk]} + \Delta H_f[InN]$, being $\Delta H_f[InN]$ the enthalpy of formation of InN. From this, we estimate a value of -271.4 eV/atom for μ_N . For the three impurities, the upper limit of the chemical potential (so that each impurity is likely to be incorporated in the host) is obtained from either the energy of the elemental bulk phase of the impurity or from the formation of a stable phase between the impurity with the elements of the host material (solubility limiting phase). For C, μ_C (-155.50 eV/atom) was derived by bulk diamond (64-atom diamond supercell) as no indium carbides compound

have been reported in InN growth. For the case of H, for In-rich conditions, we set $\mu_H = \mu_{H[H_2]}$ (-15.27 eV/atom), contrarily to N-rich conditions for which $\mu_H = \mu_{H[NH_3]}$, in accordance to Van de Walle and Neugebauer.²² For the oxygen impurity, the formation of In_2O_3 was reported during the synthesis of InN.²³ That is why μ_O is calculated from an 80-atom cubic-bixbyite In_2O_3 supercell (-434.7 eV/atom) by

$$\mu_{O[InN]} = \frac{1}{3}\mu_{In_2O_3[bulk]} - \frac{2}{3}\mu_{In[InN]}. \quad (3)$$

As it can be seen in Fig. 3, C_N possesses the highest E_{form} for most of E_F values. Similarly to the case of GaN⁸ and InN,⁹ C_N in InGaN MLQW behaves as an acceptor over a wide range of E_F values. Furthermore, in accordance to Fig. 2(b), a transition level can also be observed at 0.1 eV above E_V . This is much shallower than the one found in GaN ($E_V + 0.9$ eV)⁸ but closer to that occurring in InN at <0.5 eV above E_V . The effects of carbon on device performance are controversial. On one hand, carbon is detrimental for devices and the reduction of the carbon incorporation (by using appropriate precursors like triethylgallium) leads to improvement of the performance of InGaN photodetectors.²⁴ On the other hand, intentional incorporation of carbon, leading to n-type doping compensation, can improve the breakdown characteristics of InGaN-based HEMT-LED devices.²⁵

Next, H_N has a lower E_{form} than C_N . For both GaN and InN, H is reported to be a donor impurity^{11,18} and this is also the case for InGaN MLQW. However, H_N shares more similarities with InN rather than with GaN, as H_N is found to be a double donor just like in the case of InN. However, unlike InN and consistently with Fig. 2(c), a transition level is present in the Kohn-Sham E_{GAP} at $E_V + 0.08$ eV meaning that the double donor character of H_N in InGaN MLQW is displayed over a very limited range of E_F . As mentioned earlier, it was reported that H in InN is more stable at an interstitial site rather than at a substitutional site. Consistently to the results of Janotti,¹⁰ our calculated E_{form} for H in an interstitial bond-center configuration, H_i (not shown here) is lower than that of H_N but higher than O_N .

Regarding O_N , this impurity behaves as a donor in InGaN MLQW, for all values of E_F , as in GaN⁹ and InN.²⁶ It has also the lowest E_{form} of all the other impurities

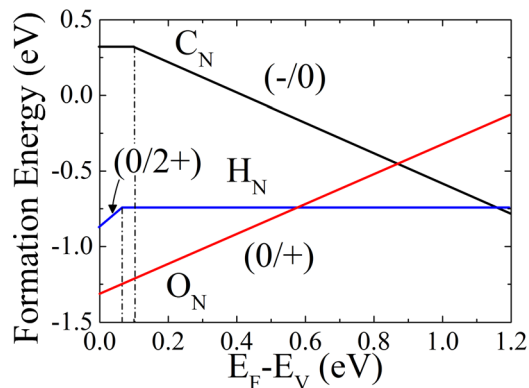


FIG. 3. Formation energy for the isolated C_N , H_N , and O_N substitutional impurities shown in the underestimated LDA band gap. Dashed lines are a guide for the eye and show the position of the transition levels in the band gap.

considered in the present study, for $E_F \leq E_V + 0.6$ eV, suggesting that, if oxygen impurities are present during growth, they will be spontaneously incorporated into the crystal making it difficult to obtain p -type InGaN. Since the growth of In-rich p -type InGaN is crucial for the development of opto-electronic devices, in the following we will focus our discussion on O_N .

The electronic structure of O_N was investigated by employing the defect-molecule model. The oxygen atom binds to one Ga atom and three In atoms (In_3GaO), as shown in Fig. 1(d). By removal of a N atom, the N vacancy (V_N) has three electrons. To these, the six electrons of oxygen need to be added. As a consequence, the In_3GaO has nine electrons in total. From the defect-molecule model, we find that the In_3GaO has a C_{3v} point symmetry, both before and after geometry relaxation. This means that the nine electrons need to be accommodated in two singlet (a_1) and one doublet (e) orbital. Since only eight electrons can be placed in two a_1 and one e orbital, we speculate that the spare electron ends up in an anti-bonding orbital, possibly a singlet (a_1^*). As shown in Fig. 3, no transition levels are present in the Kohn-Sham E_{GAP} when O_N is present in the MLQW, so we suggest that this level may be resonant in either valence or conduction band. In order to verify if this group theoretical prediction is correct, we first show (Fig. 4(a)) the charge density contour plot of the In_3GaO molecule. We note that the charge is entirely localized on the O atom and no charge is present between Ga-O and In-O, suggesting an anti-bonding character. In addition, by considering the highest occupied molecular orbital (Fig. 4(b)), we find that this is resonant in the conduction band at $\sim E_C + 0.7$ eV, consistently with what reported in Fig. 2(d) and that the sign of the wavefunction is invariant under symmetry operations of the C_{3v} group, meaning that it can be classified as an a_1 orbital.

As our results demonstrate, the presence of O_N in an InGaN MLQW can have significant consequences. We point out that a direct comparison of the electronic properties of InGaN MLQW and $In_xGa_{1-x}N$ quasi-random alloy is feasible only for high In content.²⁷ With this in mind, we can speculate that incorporation of O_N can easily occur not only in InGaN MLQW but also in $In_xGa_{1-x}N$ alloys. For instance, in accordance to our results, Kappers *et al.*²⁸ have shown that excess In, during InGaN growth, leads to a high

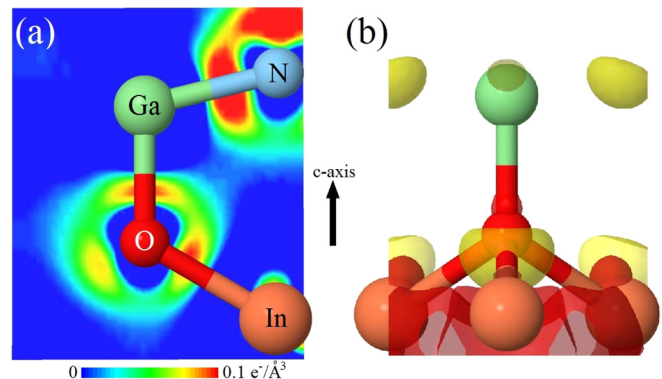


FIG. 4. (a) Charge density plot of the In_3GaO molecule, as obtained from the defect-molecule model and (b) isosurface of the calculated wave function for the same molecule (0.095 e/Å³). The red (yellow) isosurface represents the positive (negative) values of the wave function.

concentration of incorporated oxygen. Oxygen has also proven to be detrimental for the growth of strongly p -type doped $\text{In}_x\text{Ga}_{1-x}\text{N}$: indeed, it was reported²⁹ that achieving heavily doped p -type $\text{In}_x\text{Ga}_{1-x}\text{N}$ is challenging due to the presence of donor impurities. As our study shows, H_N and O_N are both donors, but O_N may be held accountable for this problem due to its lower E_{form} . Furthermore, several reports have shown that the presence of oxygen can degrade the performance of InGaN/GaN LED^{3,4} and attributed this to the incorporation of oxygen into the Mg-doped GaN, leading to high-resistivity GaN. To support this hypothesis, Poblenz *et al.*³⁰ have reported oxygen incorporation in MBE-grown $\text{In}_x\text{Ga}_{1-x}\text{N}$ and found that the oxygen content is three times higher in $\text{In}_x\text{Ga}_{1-x}\text{N}$ than in GaN for a growth temperature of 600 °C or ten times higher if the growth temperature is raised up to 750 °C.

In conclusion, we showed that oxygen is the most abundant impurity found in InGaN MLQW due to its low E_{form} and, in the high In content limit, it may also be in $\text{In}_x\text{Ga}_{1-x}\text{N}$ alloys. The E_{form} of O_N in InGaN MLQW is found to be comparably low as that of O_N in either GaN or InN, meaning that avoiding oxygen incorporation in an InGaN MLQW is crucial for the correct functionality of InGaN opto-electronic devices.

This study was partially supported by the Japanese grant KAKEN (Project No. 24560014).

¹P. G. Moses, M. S. Miao, Q. M. Yan, and C. G. van de Walle, *J. Chem. Phys.* **134**, 084703 (2011).

²M. S. Miao, Q. M. Yan, and C. G. Van de Walle, *Appl. Phys. Lett.* **102**, 102103 (2013).

³C. H. Kuo, S. J. Chang, Y. K. Su, and J. F. Chen, *IEEE Electron Device Lett.* **23**, 240 (2002).

⁴N. Okada, K. Tadatomo, K. Yamane, H. Mangyo, Y. Koabayashi, H. Ono, K. Ikenaga, Y. Yano, and K. Matsumoto, *Jpn. J. Appl. Phys., Part 1* **53**, 081001 (2014).

⁵S. Valdeza-Felip, L. Rigutti, F. B. Naranjo, B. Lacroix, S. Fernandez, P. Ruterana, F. H. Julien, M. Gonzalez-Herraez, and E. Monroy, *Phys. Status Solidi A* **209**, 17 (2012).

⁶A. Yoshikawa, S. B. Che, W. Yamaguchi, H. Saito, X. Q. Wang, Y. Ishitani, and E. S. Hwang, *Appl. Phys. Lett.* **90**, 073101 (2007).

⁷P. E. D. Soto Rodriguez, V. J. Gomez, P. Kumar, E. Calleja, and R. Nötzel, *Appl. Phys. Lett.* **102**, 131909 (2013).

⁸J. L. Lyons, A. Janotti, and C. G. Van de Walle, *Appl. Phys. Lett.* **97**, 152108 (2010).

⁹X. M. Duan and C. Stampfl, *Phys. Rev. B* **79**, 035207 (2009), and references therein.

¹⁰A. Janotti, APS March Meeting, 16–20 March 2009.

¹¹A. Janotti and C. G. Van de Walle, *Appl. Phys. Lett.* **92**, 032104 (2008).

¹²C. G. Van de Walle and J. Neugebauer, *J. Appl. Phys.* **95**, 3851 (2004).

¹³T. Mattila and R. M. Nieminen, *Phys. Rev. B* **54**, 16676 (1996).

¹⁴J. M. Soler, J. D. Gale, A. Garcia, J. Junquera, P. Ordejon, and D. Sanchez-Portal, *J. Phys. Condens. Matter* **14**, 2745 (2002).

¹⁵N. Troullier and J. L. Martins, *Phys. Rev. B* **43**, 1993 (1991).

¹⁶D. M. Ceperley and B. J. Alder, *Phys. Rev. Lett.* **45**, 566 (1980).

¹⁷H. J. Monkhorst and J. D. Pack, *Phys. Rev. B* **13**, 5188 (1976).

¹⁸A. F. Wright, C. H. Seager, S. M. Myers, D. D. Koleske, and A. A. Allerman, *J. Appl. Phys.* **94**, 2311 (2003).

¹⁹M. Magnuson, M. Mattesini, C. Höglund, J. Birch, and L. Hultman, *Phys. Rev. B* **81**, 085125 (2010).

²⁰S. B. Zhang and J. E. Northrup, *Phys. Rev. Lett.* **67**, 2339 (1991).

²¹K. Laaksonen, M. G. Ganchenkova, and R. M. Nieminen, *J. Phys. Condens. Matter* **21**, 015803 (2009).

²²C. Van de Walle and J. Neugebauer, *J. Cryst. Growth* **248**, 8 (2003).

²³E. Kurimoto, M. Hangyo, H. Harima, M. Yoshimoto, T. Yamaguchi, T. Araki, Y. Nanishi, and K. Kisoda, *Appl. Phys. Lett.* **84**, 212 (2004).

²⁴K. H. Lee, P. C. Chang, S. J. Chang, and S. L. Wu, *J. Appl. Phys.* **110**, 083113 (2011).

²⁵C. Liu, Z. Liu, T. Huang, J. Ma, and K. M. Lau, *J. Cryst. Growth* **414**, 243 (2015).

²⁶A. F. Wright *J. Appl. Phys.* **98**, 103531 (2005).

²⁷G. Staszczak, I. Gorczyca, T. Suski, X. Q. Wang, N. E. Christensen, A. Svane, E. Dimakis, and T. d. Moustakas, *J. Appl. Phys.* **113**, 123101 (2013).

²⁸M. J. Kappers, T. Zhu, S. L. Sahonta, C. J. Humphreys, and R. A. Oliver, *Phys. Status Solidi C* **12**, 403 (2015).

²⁹C. Boney, I. Hernandez, R. Pillai, D. Starikov, and A. Bensaoula, in *35th IEEE Photovoltaic Specialists Conference (PVSC)* (2010), p. 2522.

³⁰C. Poblenz, T. Mates, M. Craven, S. P. DenBaars, and J. S. Speck, *Appl. Phys. Lett.* **81**, 2767 (2002).